CR energetic spectra and its evolution in helical plasma turbulence.

Yurij Fedorov[1], Milan Stehlik[2]

***Abstract*— The energetic spectra of accelerated energetic particles is investigated using kinetic equation in a statistically anisotropic helical turbulent magnetic field in the diffusion approximation. The acceleration mechanism based on the α-effect is compared with the second order Fermi acceleration [7] (cited as Paper I). The solutions of the time-dependent equation describing stochastic particle acceleration are obtained. The steady state cosmic ray energetic spectra are also derived, and the evolution of accelerated particle spectra by their approach to equilibrium state is studied. Obtained results can be useful for description of particle acceleration in solar flares, supernova remnants, galactic nuclei and other astrophysical environments.**

I. INTRODUCTION

One of known acceleration mechanisms is the acceleration of charged energetic particles in stochastic medium, especially, in the magnetohydrodynamic turbulence. For example, the second-order Fermi mechanism has application in a wide range of astrophysical objects. Into this group can be included our consideration of particle acceleration in helical MHD turbulence in which the known α-effect arise and it can possess additional (initial) acceleration for more intensive mechanism [9], [6]. In fact, the plasma velocity fluctuations $\boldsymbol{u}_1$ together with the magnetic field fluctuations $\boldsymbol{H}_1$ produce a correlation $\langle[\boldsymbol{u}_1, \boldsymbol{H}_1]\rangle/c \equiv \mathcal{E}$ (the turbulent electromotive force) which allows the system to evolve back toward a stationary state. Beside it the helicity is a source of the electric field

$$\boldsymbol{E}_{(\alpha)} = -\frac{\alpha}{c}\boldsymbol{H}_0 \tag{1}$$

along the created homogeneous MF $\boldsymbol{H}_0$ [10], [8] (α is known as the dynamo coefficient). In result, the electric field $\boldsymbol{E}_{(\alpha)}$ can accelerate the charged particles. Effectiveness of the last acceleration mechanism in helical MHD turbulence with the second-order Fermi mechanism has been discussed in Paper I. Comparison of energetic spectra of accelerated particles and their temporal evolution is goal of this contribution.

The energetic particles can experience various kind of energetic losses and/or they can also leave acceleration region as a result of diffusion or convection. These processes result in leakage of particles which have origin in the given energy region owing to acceleration. One can introduce the escape time t_e to take into account particle energetic losses. In this approximation the diffusion equation (see Eq. (10) in Paper I) takes the form [16], [13]

$$\frac{\partial N}{\partial t} - \frac{1}{p^2}\frac{\partial}{\partial p}p^2 D_p \frac{\partial N}{\partial p} + \frac{N}{t_e} = q\,\frac{\delta(p-p_0)}{p^2}\,. \tag{2}$$

The third term N/t_e stands for particle leakage. The right hand side of the equation corresponds to the continuous injection of particles with momentum p_0 and q is the particle number injected in the unit of space during the unit of time.

The momentum diffusion coefficient D_p can be written as a sum

$$D_p = D_F + D_K\,, \tag{3}$$

where

$$D_F = \frac{p^2\langle u_1^2\rangle}{3v\Lambda}\,, \quad D_K = \alpha^2\frac{p^2\Lambda}{3vR_H^2}\,. \tag{4}$$

The first term D_F describes the statistical Fermi acceleration due to energetic particle scattering on moving magnetic irregularities. The second term D_K defines particle acceleration by the large-scale electric field $\boldsymbol{E}_{(\alpha)}$ arising in the turbulent medium due to α-effect. Here $R_H = pc/eH_0$ is the proton Larmour radius. The relative efficiency of α-acceleration (in comparison to the second order Fermi mechanism) for injection particle energy is given by the ratio

$$\eta = \frac{\alpha^2}{\langle u_1^2\rangle}\left(\frac{\Lambda_0}{R_{0H}}\right)^2\,, \tag{5}$$

where Λ_0, R_{0H} corresponds to the momentum p_0 of the particle injection. If the particle mean free path has power law dependence on momentum,

$$\Lambda = \Lambda_0\left(\frac{\zeta}{\zeta_0}\right)^\lambda\,, \qquad \zeta = \frac{p}{mc}\,, \tag{6}$$

where ζ defines the dimensionless particle momentum and m is the proton rest mass. Here ζ_0 corresponds to the injection momentum p_0. Then the momentum diffusion coefficient (3) related to the Fermi stochastic acceleration can be written as

$$D_F = D_{0F}\zeta^{1-\lambda}\sqrt{1+\zeta^2}\,, \quad D_{0F} = \frac{m^2c\langle u_1^2\rangle\zeta_0^\lambda}{3\Lambda_0}\,. \tag{7}$$

In the case of α-acceleration the coefficient D_K is

$$D_K = D_{0K}\zeta^{\lambda-1}\sqrt{1+\zeta^2}\,, \quad D_{0K} = \frac{m^2c\,\alpha^2\Lambda_0\zeta_0^{2-\lambda}}{3R_{0H}}\,. \tag{8}$$

Note that Eq. (2) has been used for the description of CR acceleration in various astrophysical objects. Solutions of similar equations has been applied for analysis and interpretation of solar CR spectra [13], [16], [14].

[1]MAO NASU Kiev, Ukraine, fedorov@mao.kiev.ua
[2]IEP SAS Košice, Slovakia, stehlik@saske.sk

II. STEADY STATE SOLUTION

For the mean free path defined by Eq. (6) the diffusion coefficient possesses the power law form:

$$D_p = D_0\zeta^\gamma \,. \tag{9}$$

Defining dimensionless time,

$$\tau = \frac{t}{t_0}\,, \qquad t_0 = \frac{(mc)^2}{D_0}\,, \tag{10}$$

the equation (2) reads

$$\frac{\partial N}{\partial \tau} - \frac{1}{\zeta^2}\frac{\partial}{\partial \zeta}\zeta^{(2+\gamma)}\frac{\partial N}{\partial \zeta} + \frac{N}{\tau_e} = qt_0\frac{\delta(\zeta-\zeta_0)}{(mc)^3\zeta^2}\,. \tag{11}$$

The quantity τ_e equals to the ratio of the escape time t_e to the acceleration time t_0 in (10):

$$\tau_e = \frac{t_e}{t_0}\,. \tag{12}$$

Let the escape time from the acceleration region is independent on CR energy ($t_e = const$). Such approximation has been used, for example, in [13]. Some authors took also the energetic dependence of t_e into considerations (see e.g. [3]). The equilibrium CR energetic spectrum arises provided the number of accelerated particles of given energy is equal to the number of particles leaving acceleration region. In that case the time derivative in the left hand side of Eq. (11) can be neglected what gives the stationary equation. Analogously to the solutions of the non-stationary equation in Paper I similar expressions can be derived for steady state solutions. In result,

$$\begin{aligned} N(\zeta) &= \frac{qt_0}{\tilde{\gamma}(mc)^3}\exp\left[-\frac{1+\gamma}{2}\ln(\zeta\zeta_0)\right] \\ &\times K_\nu\left(\frac{\exp\left[\tilde{\gamma}\ln(\zeta_0)\right]}{\tilde{\gamma}\sqrt{\tau_e}}\right) I_\nu\left(\frac{\exp\left[\tilde{\gamma}\ln(\zeta)\right]}{\tilde{\gamma}\sqrt{\tau_e}}\right) \end{aligned} \tag{13}$$

for $\zeta < \zeta_0$, and

$$\begin{aligned} N(\zeta) &= \frac{qt_0}{\tilde{\gamma}(mc)^3}\exp\left[-\frac{1+\gamma}{2}\ln(\zeta\zeta_0)\right] \\ &\times I_\nu\left(\frac{\exp\left[\tilde{\gamma}\ln\zeta_0\right]}{\tilde{\gamma}\sqrt{\tau_e}}\right) K_\nu\left(\frac{\exp\left[\tilde{\gamma}\ln\zeta\right]}{\tilde{\gamma}\sqrt{\tau_e}}\right) \end{aligned} \tag{14}$$

for $\zeta > \zeta_0$. Here $\tilde{\gamma} = (2-\gamma)/2$ and $\nu = (1+\gamma)/(2-\gamma)$. From the last solution one obtain the expression for the density of high energy particles:

$$N(\zeta) \propto \zeta^{-1-\frac{\gamma}{4}}\exp\left(-\frac{\exp\left[\tilde{\gamma}\ln\zeta\right]}{\tilde{\gamma}\sqrt{\tau_e}}\right)\,. \tag{15}$$

So, the particle density exponentially decreases with energy. The solutions (13),(14) are valid only if $\gamma \neq 2$. In fact, when exponent γ approach to 2 the index ν increases indefinitely. This particular case need a special examination, as follows below.

Let us consider the stochastic Fermi acceleration of particles having the constant mean free path ($\lambda = 0$). In the nonrelativistic energy region the diffusion coefficient D_p in (7) is proportional to momentum that $\gamma = 1$. Setting $\nu = 2$ in expression (14) one obtain the known expression for nonrelativistic CR density [13], [14]

$$N(\zeta) = \frac{2qt_0}{(mc)^3}\frac{1}{\zeta\zeta_0}I_2\left(2\sqrt{\frac{\zeta_0}{\tau_e}}\right)K_2\left(2\sqrt{\frac{\zeta}{\tau_e}}\right)\,. \tag{16}$$

The momentum diffusion coefficient (7) for ultrarelativistic particles, in considered case of $\Lambda = const$, is proportional to ζ^2. Thus one has to solve the equation (11) with $\gamma = 2$. This solution takes the known form [13], [14]

$$N(\zeta) = \frac{qt_0}{2(mc)^3\sqrt{\frac{1}{\tau_e}+\frac{9}{4}}}\left(\frac{\zeta}{\zeta_0}\right)^{\Gamma_u}\,,\ \Gamma_u = -\frac{3}{2} - \sqrt{\frac{1}{\tau_e}+\frac{9}{4}} \tag{17}$$

with the power law dependence of ultrarelativistic CR density on particle momentum.

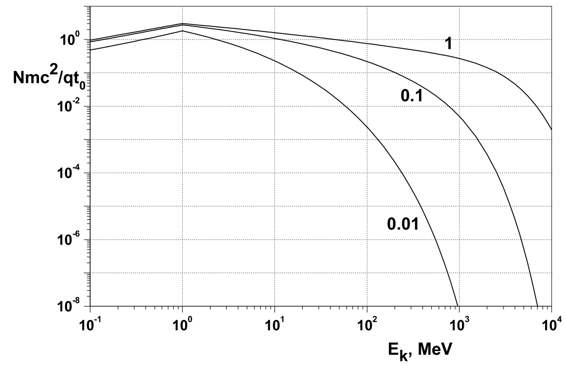

Fig. 1. The steady state energetic distribution for $\lambda = 0.5$ and $\varepsilon_{k0} = 1$ MeV. The case of Fermi acceleration.

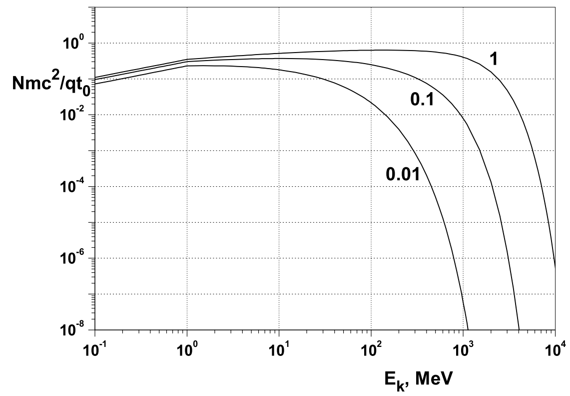

Fig. 2. As in Fig. 1 in the case of α-acceleration.

Now let us consider the steady state CR energetic spectra. If the function $N(\zeta)$ is known, one can make the change of variable ζ to kinetic energy using relationship

$$N(\varepsilon_k) = \frac{p^2}{v}N(p) = \frac{(mc)^2\zeta^2}{v}N(\zeta)\,, \tag{18}$$

where v is the particle velocity and the dimensionless momentum is associated with kinetic energy according to

$$\zeta = \frac{\sqrt{\varepsilon_k(\varepsilon_k+2mc^2)}}{mc^2}\,. \tag{19}$$

The CR steady state energetic spectra calculated according to (13),(14),(18) is shown in Fig. 1. These spectra correspond to statistical Fermi acceleration of particles with the $\Lambda \propto \sqrt{p}$ ($\lambda = 0.5$). Numbers near curves denote value τ_e of the relative rate of particle escape out of the acceleration region. The injected particle kinetic energy equals to 1 MeV and the exponent γ of the diffusion coefficient (9) is 0.5. The CR spectrum in high energy region (above the injected energy) prove to be harder with the escape time increase (Fig. 1) [13].

Now let us consider the steady state energetic spectrum typical for α-acceleration. We will exploit the same momentum dependence of mean free path ($\lambda = 0.5$) as in the case of Fermi acceleration in Fig. 1. Nonrelativistic momentum diffusion coefficient D_p (8) has the form of (9) with index $\gamma = -0.5$. In Fig. 2 the dependence of normalized particle density on kinetic energy is illustrated, given by relations (13),(14),(18). Here initial proton energy is the same ($\varepsilon_k = 1$ MeV) and numbers near the curves denote τ_e. Analogically to Fig. 1 the spectrum prove to be harder for increasing escape time. In the low energy region the CR spectrum which is suitable for α-acceleration, appears to be harder then the spectrum fitted to Fermi acceleration. On the contrary the energetic distribution of high energy CR is found to be softer for particle acceleration by the large scale electric field $\boldsymbol{E}_{(\alpha)}$, Eq. (1).

III. PARTICLE ENERGETIC SPECTRA

The momentum spectrum exponent Γ can be found from formulae

$$\Gamma = \frac{\zeta}{N}\frac{\partial N(\zeta)}{\partial \zeta}\,. \tag{20}$$

For high energy particles ($\zeta > \zeta_0$) one obtain from expression (14) that

$$\Gamma(\zeta) = -\frac{1+\gamma}{2} - \frac{\exp\left[\tilde{\gamma}\ln\zeta\right]}{2\sqrt{\tau_e}}\left[K_\nu\left(\frac{2\exp\left[\tilde{\gamma}\ln\zeta\right]}{(2-\gamma)\sqrt{\tau_e}}\right)\right]^{-1} \times\left\{K_{\nu-1}\left(\frac{\exp\left[\tilde{\gamma}\ln\zeta\right]}{\tilde{\gamma}\sqrt{\tau_e}}\right) + K_{\nu+1}\left(\frac{\exp\left[\tilde{\gamma}\ln\zeta\right]}{\tilde{\gamma}\sqrt{\tau_e}}\right)\right\}. \tag{21}$$

Evidently, this expression is valid only for $\gamma \neq 2$. In the case of $\gamma = 2$ which corresponds to Fermi acceleration of ultrarelativistic particles with constant mean free path one obtain from (17) that

$$\Gamma = \Gamma_u\,, \tag{22}$$

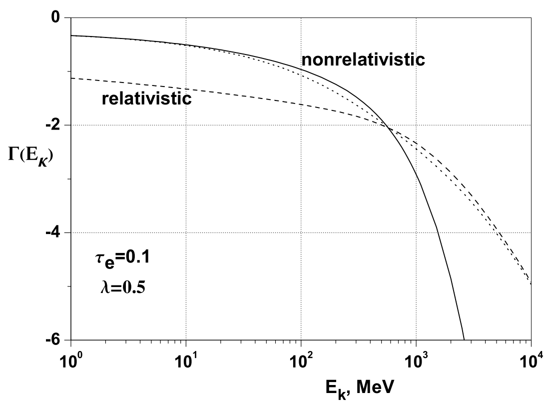

Fig. 3. The index of energetic spectrum in the steady state solution. The case of Fermi acceleration.

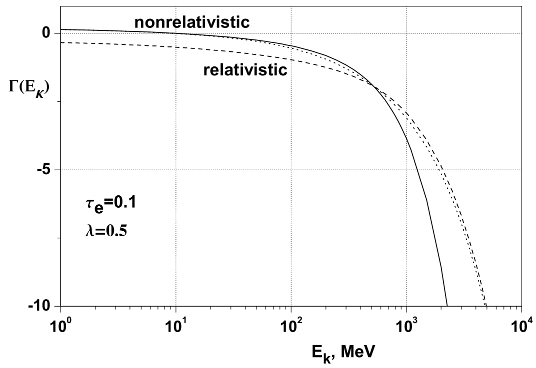

Fig. 4. As in Fig. 3 in the case of α-acceleration.

i.e. a power law momentum spectrum with exponent Γ depending on the single parameter τ_e.

The energy spectrum exponent can be calculated from formulae

$$\Gamma_{\varepsilon k} = \frac{\varepsilon_k}{N(\varepsilon_k)}\frac{\partial N(\varepsilon_k)}{\partial \varepsilon_k} \tag{23}$$

provided the momentum spectrum exponent $\Gamma_\zeta \equiv \Gamma(\zeta)$ is known:

$$\Gamma_{\varepsilon k} = \frac{\varepsilon_k + mc^2}{\varepsilon_k + 2mc^2}\left\{\Gamma_\zeta + 1 + \frac{\varepsilon_k(\varepsilon_k + 2mc^2)}{(\varepsilon_k + mc^2)^2}\right\}. \tag{24}$$

The spectral exponent $\Gamma_{\varepsilon k}$ as a function of kinetic energy is shown in Fig. 3 (for Fermi acceleration with D_p defined by (7)) and in Fig. 4 (for α-acceleration with D_p defined by (8)) where $\tau_e = 0.1$, $\lambda = 0.5$. The solid curves represent nonrelativistic particles and the dash curves correspond to ultrarelativistic ones. Note that nonrelativistic protons have kinetic energy of about 200 MeV (or less) and ultrarelativistic protons possess energy at least a few GeV. In the case of stochastic Fermi acceleration the exponent $\gamma = 0.5$ in (9) for nonrelativistic particles and $\gamma = 3/2$ in the ultrarelativistic region. Fig. 4 corresponds to α-acceleration with $\lambda = 0.5$, therefore, the exponent γ in (9) equals $\gamma = -0.5$ for nonrelativistic particles and $\gamma = 0.5$ for ultrarelativistic ones. One can see that for $\tau_e = 0.1$; $\lambda = 0.5$ the curves which correspond to nonrelativistic and ultrarelativistic protons intersect one another at kinetic energy about $\varepsilon_{k1} \simeq 500$ MeV in Figs. 3-4. In the low energy region $\varepsilon_k < \varepsilon_{k1}$ the exponent $\Gamma_{\varepsilon k}$ of nonrelativistic particles is bigger, but on the contrary for $\varepsilon_k > \varepsilon_{k1}$ value of the exponent of ultrarelativistic particles exceeds the corresponding value of nonrelativistic ones.

The dependence of spectrum exponent $\Gamma_{\varepsilon k}$ on kinetic energy coincides with the solid curve (in Figs. 3-4) in nonrelativistic region and with the dash curve for ultrarelativistic particles. If the particle energy increases the spectrum exponent passes gradually from solid curve to the dash ones. It is worth to note that the steady state proton spectrum in the transrelativistic energy region has been obtained in [16]. Let us consider the particle acceleration in the transrelativistic region. Here the diffusion coefficients (7),(8) do not have a power law form (9) even for the simple momentum dependence of the mean free path (6). From expressions (7),(8) follows that the exponent γ of diffusion coefficient (9) increases by unity between nonrelativistic and ultrarelativistic region. Defining the power exponent in (9) by formulae

$$\gamma(\zeta) = \frac{\zeta}{D_p(\zeta)} \frac{\partial D_p(\zeta)}{\partial \zeta} \tag{25}$$

in the total energy range one obtains correct γ value for nonrelativistic as well as for ultrarelativistic particles. Then the steady state solution (13),(14) can be used to calculate CR spectra. In fact, this solution is rigorously correct only for constant value of γ. In considered approximation the expression for momentum spectrum exponent $\Gamma(\zeta)$ was exploited in all CR energy region where $\gamma(\zeta)$ is given by (25). These approximate values of spectrum exponent (21),(24) are shown in Figs. 3-4 as a dotted curves. It is seen from these figures that exponent $\Gamma_{\varepsilon k}$ is monotonically decreasing function of kinetic energy meanwhile the dotted curves coincides with solid ones for nonrelativistic protons and they approach dash curves corresponding to ultrarelativistic CR.

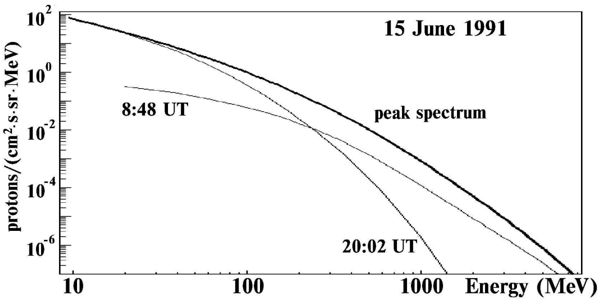

Fig. 5. The SCR energetic spectrum near the Earth [4].

The developed approach can be used for the analysis and interpretation of energetic spectra of protons accelerated during solar flares. However it is necessary to take into account that derivation of Eq. (2) supposed the angular CR distribution be near isotropic. The GLE of 1991, June 15, has SCR distribution near to isotropic almost from the very beginning of the event (the lanch of the GLE was at 08:10 UT) [?]. The energetic spectrum of SCR of this observed event near the Earth became softer with the lapse of time [1], [4]. This spectrum is presented in Fig. 5 (pick over [4]) for two instants of time. It is clearly seen that in the beginning of event (at 08:48 UT) the spectrum is depleted by low energy particles, but later the SCR distribution become softer due to the fact of high energy particles rapidly leave the given volume. The peak spectrum of this GLE is depicted which prove to be close to the particle spectrum in the acceleration region [1], [4]. The solid line in Fig. 6 represents the exponent of spectrum in the GLE as a function of proton kinetic energy [4]. This exponent $\Gamma_{\varepsilon k}$ meets the SCR peak spectrum shown in Fig. 5. The dash curve presents the exponent calculated by (21, 24) where γ is given by (25) supposing that the mean free path is independent on kinetic energy ($\lambda = 0$) and the time of escape τ_e equals to 0.03. The calculated value of $\Gamma_{\varepsilon k}$ in low energy region (≤ 300 MeV) appears to be greater than the observed value (solid line in Fig. 6).

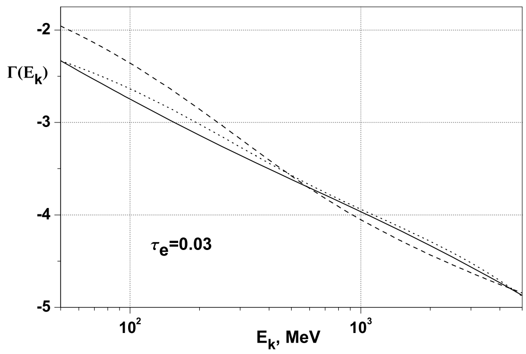

Fig. 6. The calculated spectral index for the event of Fig. 5.

The coincidence is better when the parameter λ in (6) depends on energy. According to experimental data the exponent of the rigidity spectrum can often be presented as a linear function of the logarithm of rigidity [?]. Similarly one can take also λ to be linear function of $\ln \zeta$:

$$\lambda(\zeta) = \lambda_0 + \lambda_1 \ln \frac{\zeta}{\zeta_0} , \tag{26}$$

where λ_0 corresponds to dimensionless momentum of injected particles, ζ_0. In this approximation the value of γ, Eq. (25), depends on parameters λ_0, λ_1 entering the formula (26). The dotted curve in Fig. 6 represents the spectrum index $\Gamma_{\varepsilon k}$ by (21),(24) taking into account the mean free path given by (6, 26). Note that under selected set of parameters $\lambda_0 = -0.3, \lambda_1 = 0.1$ the mean free path decreases with energy in low energy region and Λ is virtually constant at $\varepsilon_k \geq 1$ GeV.

Alternative mechanism of CR acceleration appears to be an acceleration process on astrophysical shock waves [14], [5], [11], [15]. In such kind of acceleration the particle concentration prove to be a power law function of momentum and the spectral exponent is defined by the medium compression ratio. Number of effects result in the steepening of the spectrum in the high energy region [5], [12]. Certain SCR flares can be interpreted as a consequence of either stochastic acceleration or shock wave acceleration. For example, in the paper [5] the SCR spectrum in the event on November 28, 1972 has been explained on the frame of shock acceleration mechanism. On the contrary according to our calculations this spectrum can be caused by stochastic particle acceleration when $\tau_e = 0.002$ and $\lambda = 0.5$. The proton event on May 7, 1978, has been characterized by the rather hard spectrum with steepening at proton kinetic energy of 5 GeV [5], [12]. Following our calculation this spectrum can be explained not only by the shock acceleration but also by stochastic proton acceleration in solar corona. The solar proton event on February 16, 1984, shows the power law rigidity spectrum of SCR up to the kinetic energy of the order of 10 GeV [Loc.etc.90].

It is necessary to note that we failed to interpret this SCR momentum distribution as a result of stochastic acceleration. Evidently the crucial significance for the GLE on February 16, 1984 has the energetic particle acceleration by shock waves propagated in solar corona [12].

IV. EVOLUTION OF ENERGETIC SPECTRA

Let us consider the evolution of particle momentum distribution starting from time - dependent equation (11). It is convenient to use the Laplace transform

$$\Phi(\zeta, s) = \int_0^\infty \mathrm{d}\tau\, \mathrm{e}^{-s\tau} \Phi(\zeta, \tau) \tag{27}$$

for the new distribution function

$$\Phi(\zeta, \tau) = N(\zeta, \tau) \exp\left(\frac{\tau}{\tau_e}\right). \tag{28}$$

The function (27) has to be continuous at $\zeta = \zeta_0$ (ζ_0 - the dimensionless momentum of injected particles) and its derivative on ζ at the point ζ_0 has to satisfy the condition provided by the existence of particle source in (11):

$$\frac{\partial\Phi(\zeta_0 + 0, s)}{\partial\zeta} - \frac{\partial\Phi(\zeta_0 - 0, s)}{\partial\zeta} = -\frac{t_0 q \zeta_0^{-2-q}}{(mc)^3 (s - \tilde{\gamma}^2/\tau_e)} \tag{29}$$

where $\tilde{\gamma} = (2-\gamma)/2$. This condition at $\zeta = \zeta_0$ is satisfied by the solution

$$\Phi(\zeta, s) = \frac{t_0 q}{\tilde{\gamma}(mc)^3} \frac{(\zeta\zeta_0)^{-\frac{1+\gamma}{2}}}{(s - \tilde{\gamma}^2/\tau_e)} K_\nu\left(\sqrt{s}\zeta_0^{\tilde{\gamma}}\right) I_\nu\left(\sqrt{s}\zeta^{\tilde{\gamma}}\right) \tag{30}$$

for $\zeta < \zeta_0$, and

$$\Phi(\zeta, s) = \frac{t_0 q}{\tilde{\gamma}(mc)^3} \frac{(\zeta\zeta_0)^{-\frac{1+\gamma}{2}}}{(s - \tilde{\gamma}^2/\tau_e)} K_\nu\left(\sqrt{s}\zeta^{\tilde{\gamma}}\right) I_\nu\left(\sqrt{s}\zeta_0^{\tilde{\gamma}}\right) \tag{31}$$

for $\zeta > \zeta_0$. Parameter γ defines momentum dependence of the diffusion coefficient $D_p(\zeta)$ in (9) and the index of Bessel functions $\nu = (1+\gamma)/(2-\gamma)$. Inverse Laplace transform [**?**] and using of (28) yields

$$N(\zeta, \tau) = \frac{q t_0}{(2-\gamma)(mc)^3} (\zeta\zeta_0)^{-\frac{1+\gamma}{2}} \tag{32}$$

$$\int_0^{\tilde{\tau}} \frac{\mathrm{d}\xi}{\xi} \exp\left[-\frac{\xi}{\tilde{\gamma}^2\tau_e} - \frac{\zeta^{2-\gamma} + \zeta_0^{2-\gamma}}{4\xi}\right] I_\nu\left(\frac{(\zeta\zeta_0)^{\tilde{\gamma}}}{2\xi}\right),$$

where the upper limit of integration is $\tilde{\tau} = \tilde{\gamma}^2\tau$.

Fig. 7 shows the dependence of the normalized particle density on proton kinetic energy. The time - dependent density has been calculated using (18),(32) for following parameters: $\gamma = 0.5; \tau_e = 0.1; \varepsilon_{k0} = 1$ MeV. The value of γ corresponds to $\lambda = 1/2$ in (6) in the case of Fermi acceleration of nonrelativistic particles. Number near curves represent the dimensionless time $\tau = t/t_0$ where t_0 is given by (10). The dash curve corresponds to the steady state solution (13),(14),(18). One can see that the particle number of given energy approaches the steady state value in large time limit, therefore, the spectrum evolve gradually to this equilibrium energetic distribution.

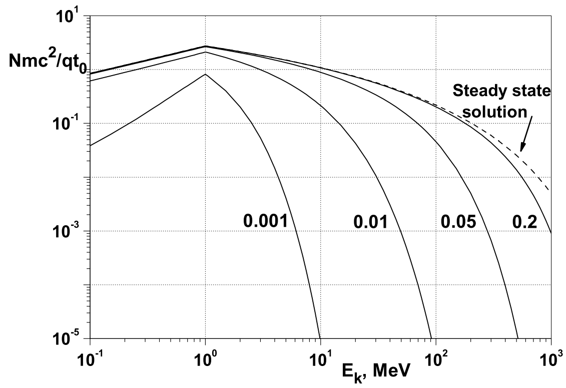

Fig. 7. The energy spectrum evolution. The case of Fermi acceleration.

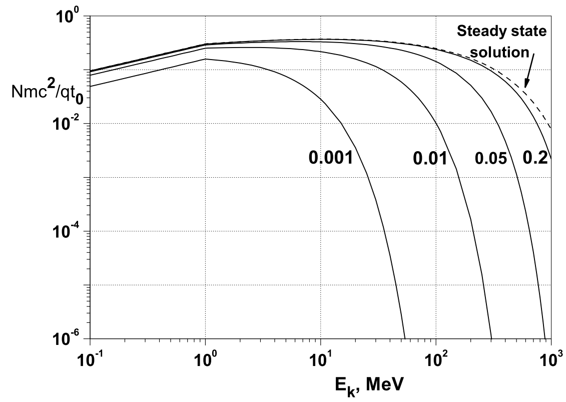

Fig. 8. As in Fig. 7 in the case of α-acceleration.

The evolution of the spectra (under continuous particle injection) is illustrated in Fig. 8 in the case of the α-acceleration. Here $\gamma = -0.5; \tau_e = 0.1; \varepsilon_{k0} = 1$ MeV. This value of γ relates to $\lambda = 1/2$ for nonrelativistic particles accelerated by electric field (1). Numbers near solid curves are equal to τ and the dash curve represents the equilibrium spectrum. For example, in the instant $\tau = 0.05$ the spectrum is closed to the equilibrium one for $\varepsilon_k \leq 10$ MeV. At $\tau = 0.2$ the spectrum virtually match up to proton kinetic energy $\varepsilon_k \simeq 200$ MeV.

The derived expressions allow to estimate the typical time of CR spectrum approaching to the equilibrium energetic distribution. Previously the magnitude of specific acceleration time about 6 seconds has been used in (10),(7) for the initial kinetic energy $\varepsilon_{k0} = 1$ MeV and $\lambda = 0.5$. Let one choices physical properties of the acceleration region, $H_0 = 100$ gauss, $\Lambda_0 = 100\, R_0$, $u_1 = 10^8$ cm/sec [5], [13], [2], [12]. Then calculation in the case of Fermi acceleration with the diffusion coefficient (4) and the escape time $\tau_e = 0.1$ gives at instant 3 second (past their injection) the number of particles of $\varepsilon_k = 1$ GeV differing from the equilibrium value less than $\approx 5\%$. The energy of continuously injected particles was $\varepsilon_{k0} = 1$ MeV in calculation of the equilibrium spectrum. The acceleration time for protons of $\varepsilon_k = 100$ MeV will be roughly equal to one second (see in Fig. 7). The steady state CR spectrum is formed rapidly when the intensity of particle escape from the acceleration region is bigger. For example, if $\tau_e = 0.01$, the particle number of 1 GeV protons coincides with the equilibrium value (of $\approx 5.10^{-2}$) past 1 second of continuous injection of 1 MeV protons. Roughly the same values of typical acceleration times has been calculated in the case of α-acceleration for the parameter $\eta = 10$ (which characterizes relative efficiency of this acceleration mechanism, see Eq. (5)). Note that these obtained values of acceleration times sufficiently good agree with both the observational data and the known consideration of energetic particle statistical acceleration [5], [13], [2], [14].

V. CONCLUSION

The steady state solutions of equation describing particle acceleration are derived and these solutions are applied to the analysis of solar cosmic ray spectra. The time - dependent solutions are investigated and the typical acceleration times are estimated. It was shown that typical acceleration time (from proton kinetic energy $\varepsilon_{k0} = 1$ MeV up to 1 GeV) for solar coronal active regions has the order of magnitude of one or a few seconds. The obtained results can be useful for description of statistical acceleration in solar flares, supernova remnants, galactic nuclei and other astrophysical environments.

ACKNOWLEDGEMENTS

This work was supported by Science and Technology Assistance Agency under the contracts APVV-0538, and by SAS, projects No. 2/7063 and No. 2/6193.

REFERENCES

[1] V.V.Akimov, P.Ambroz, A.V.Belov, et al. 1996, Solar Phys. **166**, 107.
[2] M.J.Aschwanden. 2002, Sp.Sci.Rev. 101, 1.
[3] P.A.Becker, T.Le, C.D.Dermer. 2006, ApJ. 647, 539.
[4] A.V.Belov, E.A.Eroshenko. 1996, Adv.Space Res. 17, 167.
[5] D.C.Ellison, R.Ramaty. 1985, ApJ. **298**, 400.
[6] Yu.I.Fedorov, M.E.Katz, L.L.Kichatinov, M.Stehlik. 1992, AA. **260**, 499.
[7] Yu.I.Fedorov, M.Stehlik. 2008, this conf. O3.11, (cited as Paper I).
[8] M.Hnatic, M.Jurcisin, M.Stehlik. 2001, Magnit.Gidrodin. **37**, 80.
[9] L.L.Kichatinov. 1983, Pis'ma Zh.Eksp.Teor.Fiz. **37**, 43; Proc.18th ICRC, Bangalore, 1983, v.3. p.145.
[10] F.Krause, K.-H.Rädler. *Mean-field Magnetohydrodynamics and Dynamo Theory*, New York: Pergamon Press, 1980.
[11] M.A.Lee, J.M.Ryan. 1986, ApJ. **303**, 829.
[12] J.A.Lockwood, H.Debruner, E.O.Flückiger, H.Grädel. 1990, ApJ. **355**, 287.
[13] J.A.Miller, N.Guessoum, R.Ramaty. 1990, ApJ. **361**, 701.
[14] R.Ramaty, R.J.Murphy. 1987, Sp.Sci.Rev. 45, 213.
[15] D.V.Reames. 1999, Sp.Sci.Rev. 90, 413.
[16] J.Steinacker, R.Schlickeiser. 1989, AA. 224, 259.